Supporting Information

Extremely large magnetoresistance in high quality magnetic Fe_2Ge_3 single crystals

Yuan-Qiao Chen[1], Wei-Bin Wu[1], Ya-Xun He[1], Jia-Ying Zhang[1], Tian He[1], Zhe Li[2], Qi-Ling Xiao[1]* and Jun-Yi Ge[1]**

1. *Materials Genome Institute, Shanghai University, Shanghai 200444 China*
2. *Guangdong Provincial Key Laboratory of Semiconductor Optoelectronic Materials and Intelligent Photonic Systems, School of Science, Harbin Institute of Technology (Shenzhen), Shenzhen 518055, China*

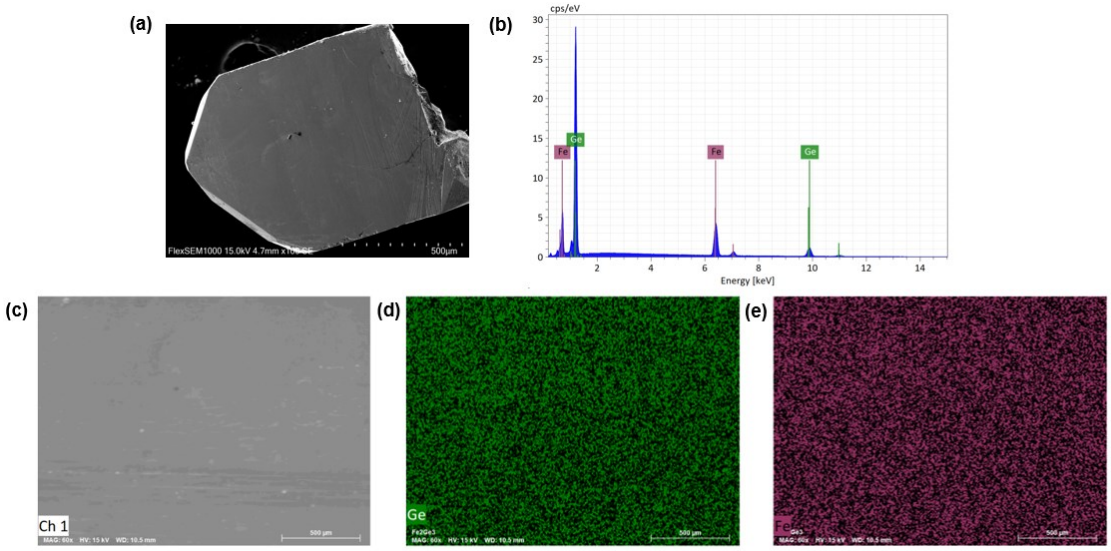

Figure S1 (a) SEM of the Fe_2Ge_3 single crystals. (b) Energy-dispersive X-ray spectroscopy of Fe_2Ge_3. (c) Surface morphology of the sample. (d), (e) Elemental distribution diagrams of Fe and Ge elements.

Figure S1a displays the scanning electron microscope image with a magnification of 100x and the surface of the sample is flat and smooth. Energy dispersive X-ray spectroscopy analysis of Fe_2Ge_3 shows that there are no impurities in the single crystal. EDS mapping shows a homogeneous composition distribution in the studied Fe_2Ge_3 crystals.

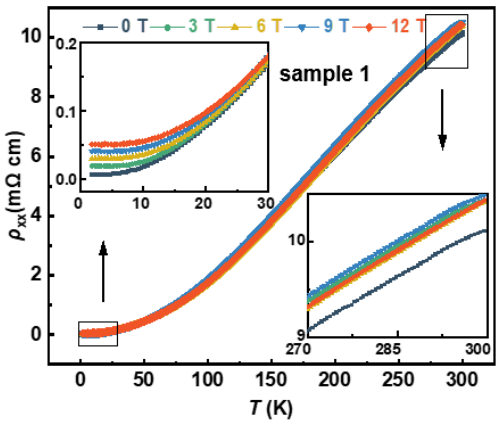

Figure S2 The temperature-dependence resistivity ρ_{xx} under external magnetic fields of 0 T, 3 T, 6 T, 9 T and 12 T. Inset: enlarged views of the low and high temperature sections.

The ρ-T curves under different magnetic fields follow the same trend as the zero-field ρ-T curve, with no metal-insulation transition behavior. From the inset of Figure S2, it can be seen that the resistivity gradually increases below 30 K in the presence of magnetic fields, meaning that the MR becomes obvious. However, the ρ-T curve reverses in the high-temperature region and the motion of the electrons in the presence of the magnetic field seems to be somehow affected, in response to the fact that the

resistivity does not change monotonically with magnetic fields. Although the resistivity change under the magnetic field is not obvious, the MR reaches up to 2000% because the resistivity at 0 T is to three decimal places.

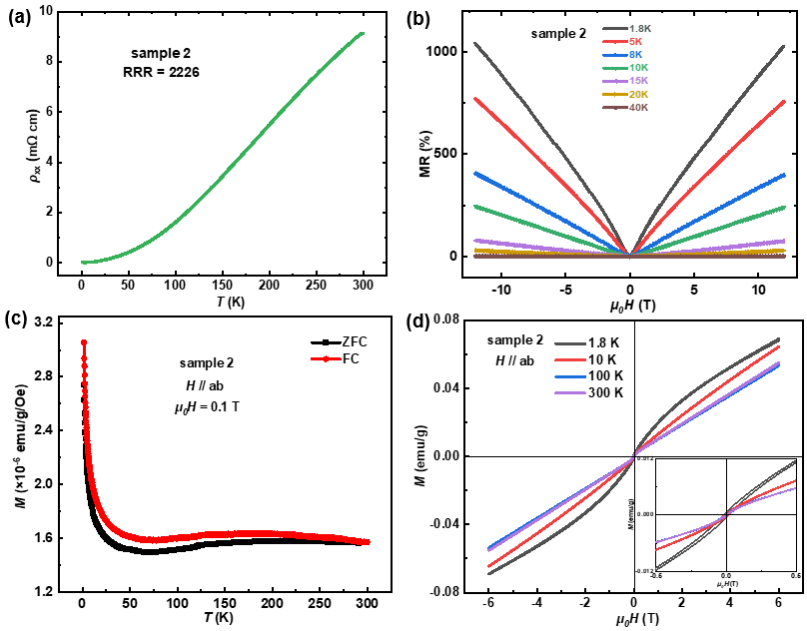

Figure S3 Electrical and magnetic transport properties of Fe_2Ge_3 sample 2. (a) Resistivity ρ_{xx} of Fe_2Ge_3 single crystal as a function of temperature. (c) Magnetic susceptibility (χ-T) curves in zero-field-cooled (ZFC) and field-cooled (FC) modes as a function of temperature. (d) Hysteresis (M-H) curves at different temperatures. The inset shows an enlarged view.

The resistivity of the Fe_2Ge_3 sample decreases with decreasing temperature, exhibiting the characteristics of a typical metallic substance. The calculated *RRR* value is 2226, indicating that the sample is of good quality with a minimal presence of impurities and defects. Similarly, the MR of Fe_2Ge_3 at 1.8 K reaches 1040%, and as the temperature increases, the MR gradually decreases, reaching 2% at 40 K. The magnetic results indicate that sample 2 continues to exhibit ferromagnetic properties. The M-H curve deviates from the expected linear trajectory, displaying a loop at both low and high temperatures.

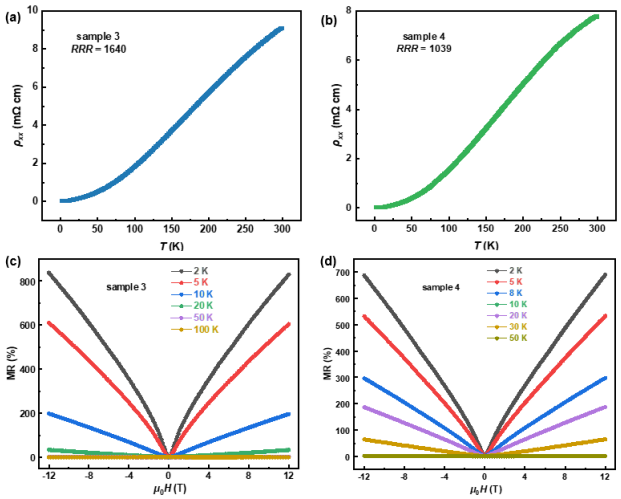

Figure S4 The temperature-dependence resistivity and MR curves of different Fe_2Ge_3 single crystals in this study. (a) and (c) depict the data for sample 3, while (b) (d) is from sample 4.

Different samples of Fe_2Ge_3 demonstrated a consistent trend of increasing resistivity with elevated temperatures and MR exhibited comparable patterns of change. The *RRR* of sample 3 reaches 1640 and MR of 830% at 2 K and 12 T, while sample 4 exhibits *RRR* of 1049 and MR of 700% under the same conditions. It is undeniable that MR is strongly dependent on the sample quality, as reflected in *RRR*, but the exact relationship between the two still needs further verification.

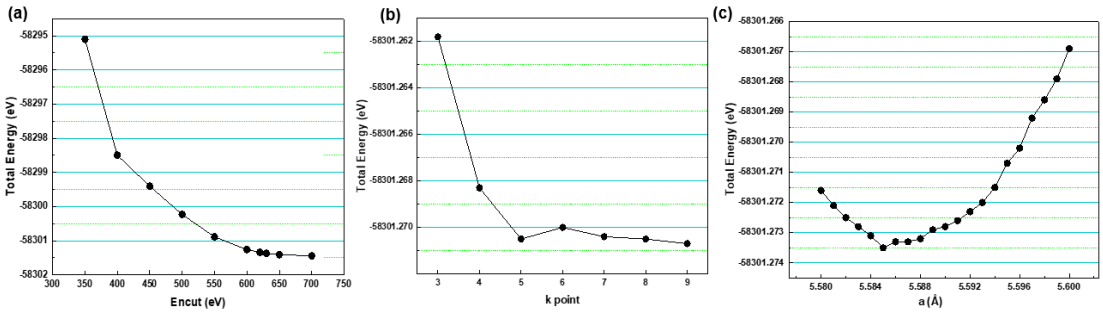

Figure S5 Convergence test before calculation of energy band structure. (a) cut-off energy. (b) k-point. (c) lattice parameter.

To ensure the accuracy of the calculated results, the parameters of the basis were tested for convergence prior to the calculation of the energy band structure. Additionally, the cut-off energy, k-point selection, and cell parameter setting, which have a significant impact on the results, were selected. In consideration of the requisite calculation time and the desired level of accuracy, the final calculation parameters are selected as follows: Energy (cut-off) = 600 eV, k-point = 5 × 5 × 5, a = b = 5.585 Å, c = 8.914 Å.

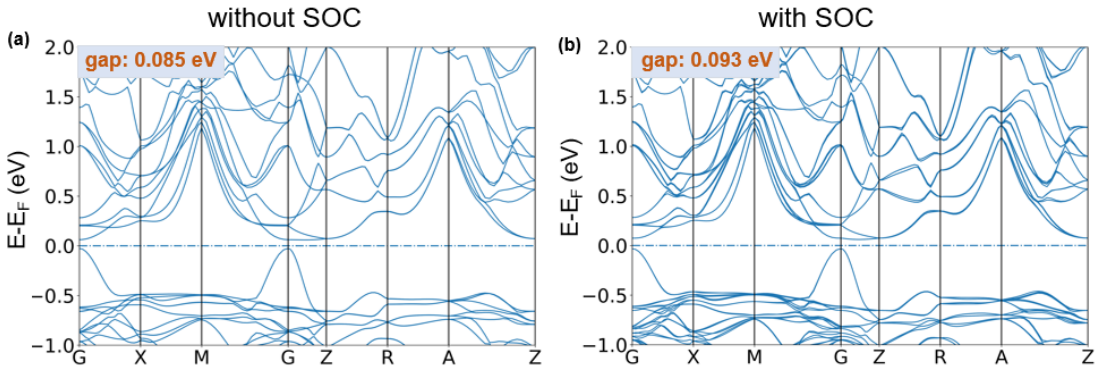

Figure S6 Electronic energy band structure of Fe_2Ge_3 obtained from first principles calculations (a) without spin–orbit coupling and (c) with spin–orbit coupling.

Figure S6 illustrate the energy band structure maps with and without spin-orbit coupling (SOC), respectively. The band gap value with SOC is 0.093 eV and it is 0.085 eV without SOC, suggesting that SOC plays a significant role in the energy band structure, especially those involving heavy elements. When SOC is taken into account, the band gap only increases by 0.01 eV, which serves to confirm that Fe_2Ge_3 is an extremely narrow-band semiconductor.

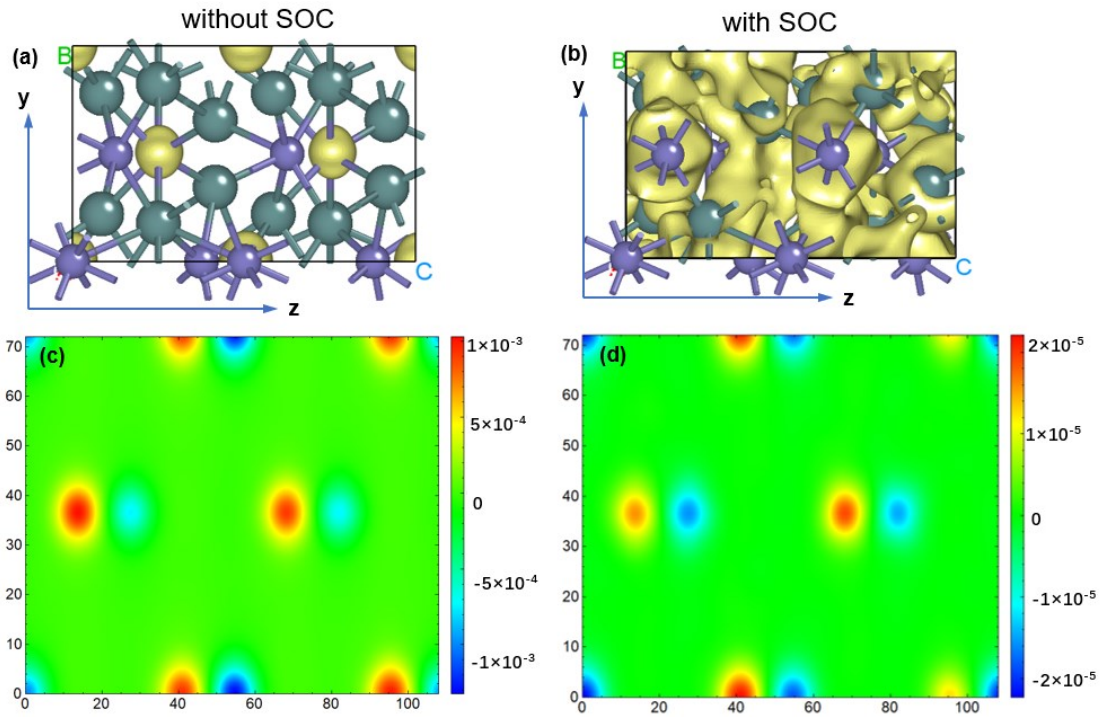

Figure S7 (a) A 3D Fourier map showing the electron density in Fe_2Ge_3. (a) A 2D Fourier map showing the electron density along the x axis. Figure (a) (c) doesn't take consideration of SOC, while (b) (d) show the same situation with SOC.

The structure appears more ordered, with well-defined electron clouds around the atomic positions when SOC is not taken into account. When SOC is included, the symmetry of the electron cloud decreases, the distribution is more complex, and the Fourier transform plot shows a decrease in peak intensity and symmetry, suggesting that SOC changes the electronic associations within Fe_2Ge_3. These Fourier transform diagrams clearly demonstrate the profound effect of SOC on electron density in Fe_2Ge_3, particularly those with strong spin-orbit interactions. The inclusion of SOC leads to a reduction in electron density modulation and introduces significant asymmetries, reflecting the complex interplay between electronic states and spin interactions.

Table S1. Crystal data and structure refinement for Fe_2Ge_3 at 293 K.

Empirical formula	Fe_2Ge_3
Formula weight	329.5 g/mol
Wavelength	0.71073 Å
Crystal system	tetragonal
Space group	*P* -4 c 2
Unit cell dimensions	a = b = 5.595(3) Å, c = 8.930(4) Å α = β = γ = 90°
Volume	279.5(2) $Å^3$
Z	4
Density (calculated)	7.8288 g/cm^3
Absorption coefficient	41.671 mm^{-1}
F (000)	592
Crystal size	0.04 × 0.03 × 0.03 mm^3
θ range for data collection	3.64 - 28.25°
Index ranges	-7 ≤ h ≤ 7, -7 ≤ k ≤ 7, -11 ≤ l ≤ 11
Reflections collected	6750
Independent reflections	354 [R_{int} = 0.0913]
Completeness to *θ* = 28.25°	100%
Refinement method	*F*
Data / restraints / parameters	354 / 0 / 26
Goodness of fit	1.36
Final *R* indices [$I > 3\sigma(I)$]	R_{obs} = 0.0264, wR_{obs} = 0.0272
R indices [all data]	R_{all} = 0.0363, wR_{all} = 0.0282
Extinction coefficient	320(30)
Largest diff. peak and hole	0.93 and -0.86 e·$Å^{-3}$

$R = \Sigma||F_o|-|F_c|| / \Sigma|F_o|$, $w_R = \{\Sigma[w(|F_o|^2 - |F_c|^2)^2] / \Sigma[w(|F_o|^4)]\}^{1/2}$ and $w = 1/(\sigma^2(F)+0.0001F^2)$

Table S2. Atomic coordinates ($x10^4$) and equivalent isotropic displacement parameters ($Å^2x10^3$) for Fe_2Ge_3 at 293 K with estimated standard deviations in parentheses.

Label	x	y	z	Occupancy	U_{eq}^*
Ge(1)	1772(2)	1772(2)	2500	1	10(1)
Ge(2)	6555(2)	2203(2)	844(2)	1	16(1)
Fe(1)	5000	5000	2500	1	8(1)
Fe(2)	0	5000	1267(3)	1	8(1)
Fe(3)	0	0	0	1	8(1)